Macromolecules

pubs.acs.org/Macromolecules Article

Synthesis of a Thermally Self-Curable Poly(styrene-*b*-isobutylene-*b*-styrene) Triblock Copolymers Using a Highly Chemoselective Divinyl Cross-Linker

Chunpeng Liu, Qingquan Liu, Yixin Liu, and Junpo He*

Cite This: *Macromolecules* 2025, 58, 9373−9386 Read Online

ACCESS | Metrics & More | Article Recommendations | Supporting Information

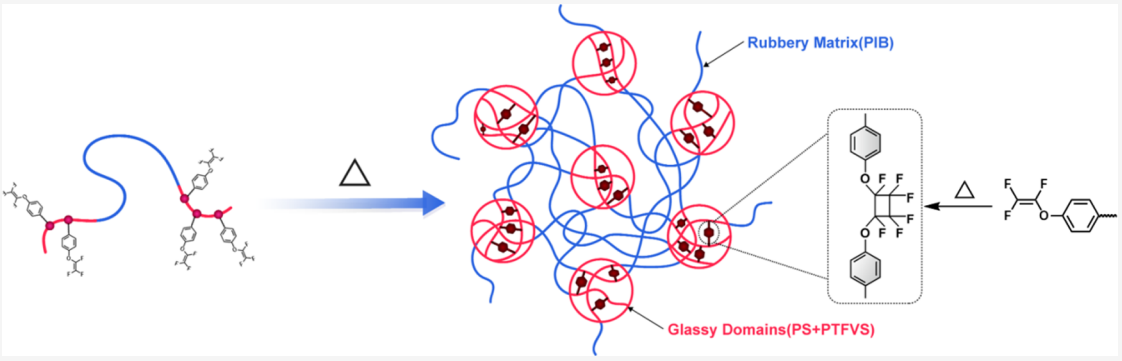

ABSTRACT: A divinyl cross-linker, 1-((1,2,2-trifluorovinyl)oxy)-4-vinylbenzene (TFVS), was synthesized and incorporated into a triblock copolymer of styrene and isobutylene (SIBS). The block copolymer was prepared through living cationic polymerization initiated with bifunctional cumyl ether in the presence of $TiCl_4$, a strategy developed by Kennedy and co-workers. Sequential feeding of monomers was applied in which isobutylene was polymerized in the first step, followed by the copolymerization of styrene and TFVS. The two vinyl groups in TFVS exhibited remarkable selectivity during cationic polymerization: the styrenic moiety readily copolymerized with styrene, while the trifluorovinyl moiety remained unreacted. The resulting triblock copolymer, poly(styrene-*co*-TFVS)-*b*-polyisobutylene-*b*-poly(styrene-*co*-TFVS), hereafter referred to as S^FIBS^F, was subject to a cross-linking reaction during molding at high temperatures (180−200 °C) through $[2\pi + 2\pi]$ thermal cycloaddition between trifluorovinyl ether moieties in polystyrene segments. The molded sample, ^{F}x-S^FIBS^F, demonstrated superior mechanical properties due to the synergistic interplay of physical and chemical cross-linking. It achieved a tensile strength of up to 30 MPa, an elastic recovery of 73.9%, and excellent creep resistance, with a maximum reduction of creep strain of 80%. These findings pave the way for the development of a new generation of polyisobutylene-based elastomers with enhanced performance and expanded application potential.

INTRODUCTION

Thermoplastic elastomers (TPEs) represent a class of triblock (ABA-type) or multiblock ($(AB)_n$ type) copolymers comprising a glassy A segment and a rubbery B segment. These copolymers undergo microphase separation due to the thermodynamic immiscibility of the constituent blocks. The resulting equilibrium morphology is typically characterized by the dispersed domains of glassy blocks within a continuous phase of rubbery segments.[1−7] These nanoscale domains serve as physical cross-linking points, establishing an elastic network by connecting rubbery blocks.[8−10] One class of conventional TPEs is the triblock copolymer of styrene, diene/isobutylene, in which polystyrene (PS) serves as the glassy segment while the rubbery segment may comprise polybutadiene (PB),[4,6,10] polyisoprene (PI),[9] and polyisobutylene (PIB).[5,7,8] These block copolymers are typically synthesized through living anionic or cationic polymerization techniques. Specifically, poly(styrene-*b*-isobutylene-*b*-styrene) (SIBS) was synthesized through the living cationic polymerization of isobutylene and styrene by sequential feeding of monomers. This technique, developed by Kennedy and co-workers, utilized dicumyl methyl ether as the initiator in conjugation with $TiCl_4$ in the presence of dimethylacetamide (DMAc) as an electron-donating additive and 2,6-di-*tert*-butylpyridine (D*t*BP) as a proton trap.[11] The use of PIB as the rubber segment endows the resulting materials with chemical stability due to its saturated hydrocarbon structure.[12−19]

Received: April 20, 2025
Revised: August 15, 2025
Accepted: August 21, 2025
Published: August 28, 2025

Scheme 1. Synthetic Route of Triblock Copolymer S^FIBS^F from Living Cationic Polymerization and the Subsequent Cross-Linking to Form ^Fx-S^FIBS^F *via* Thermal Cycloaddition

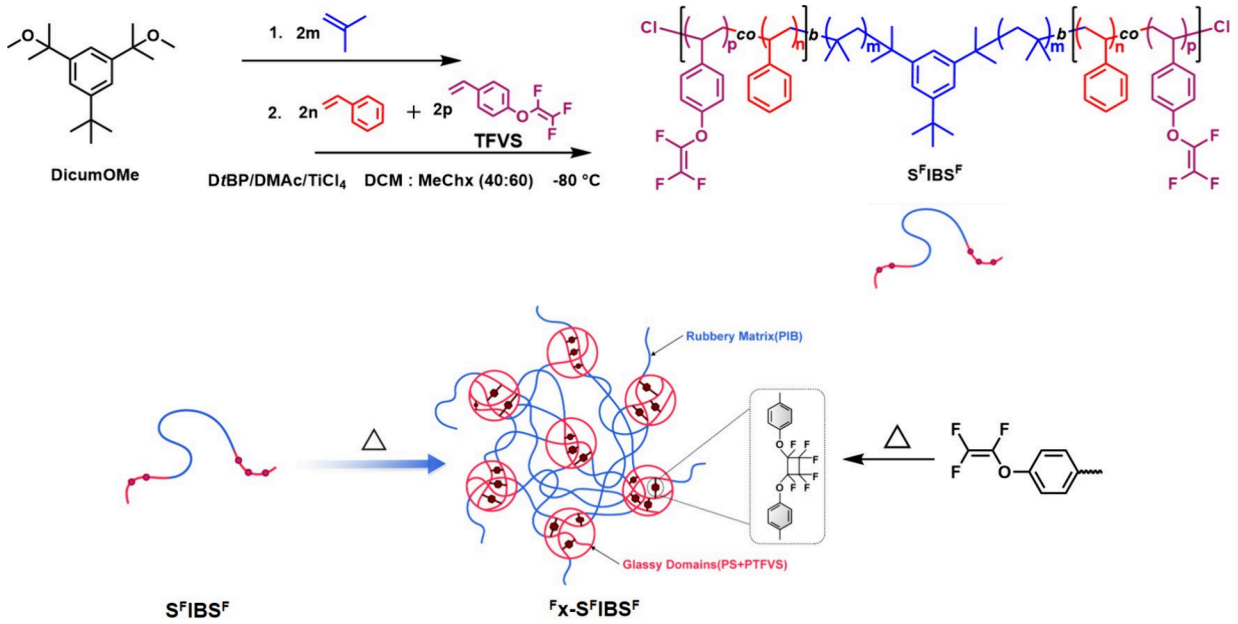

SIBS has been assessed for biomedical applications and proven to possess several desirable properties, including biostability, hemocompatibility, and resistance to infection. These characteristics make it suitable for use as an implant that does not degrade through hydrolysis, enzymolysis, or oxidation in vivo.[20−23] SIBS has been applied successfully as the coating for drug-eluting coronary stents, while other applications, such as trileaflet polymeric prosthetic heart valves (PPHV), drainage tube implants to treat glaucoma and spinal implants, are also promising.[24−29] However, one of the limitations of SIBS is its poor creep resistance, which restricts its use in load-bearing applications where long-term mechanical stability is crucial. Pinchuk et al. developed a thermoset formulation of SIBS by incorporating 4-vinylbenzocyclobutene as a cross-linker. This modification allows SIBS to undergo cross-linking via the Diels−Alder reaction between benzocyclobutene moieties during thermocompression molding. This strategy significantly enhances the mechanical properties of the molded sample, while maintaining low thrombogenicity, making SIBS a viable substrate for the development of PPHV.[30]

Trifluorovinyl ether (TFVE) is a functional group capable of undergoing $[2\pi + 2\pi]$ cyclodimerization upon heating without the need for a catalyst.[31−34] The reaction has been widely utilized to synthesize polymers containing perfluorocyclobutane (PFCB) units in their main chains, star arms, or networks through polycondensation of bifunctional monomers[34] or multifunctional monomers.[35]. The resulting PFCB-containing products exhibit exceptional properties such as thermal and chemical stability, high hydrophobicity, and low dielectric constants.[36] In the context of chain growth polymerization, (meth)acrylate monomers bearing PFCB moieties have been synthesized and subjected to controlled radical polymerization with the purpose of preparing a series of linear amphiphilic block copolymers with PFCB as side groups, which were suitable for self-assembly studies.[37−42] Additionally, a TFVE-containing (meth)acrylate monomer has been copolymerized with methyl methacrylate to produce cross-linked poly(methyl methacrylate) with enhanced thermal stability.[43] Furthermore, a variety of TFVE-functionalized organosiloxanes and polyhedral oligomeric silsesquioxanes (POSS) have been synthesized for the development of linear, star, and cross-linked organic−inorganic hybrid materials with low dielectric constants.[44−50] In another approach, poly(vinylphenol) was cross-linked via the cyclodimerization of TFVE moieties introduced through postmodification of the precursor.[51] The syntheses of TFVE-containing monomers and their polymerization strategies were summarized and discussed in a comprehensive review paper.[52]

In the present study, we synthesized a novel cross-linker, 1-((1,2,2-trifluorovinyl)oxy)-4-vinyl-benzene (TFVS), to introduce cross-links into polystyrene (PS) blocks of SIBS with the purpose of enhancing the tensile property and creep resistance. TFVS contains two distinct vinyl groups: a styrenic group and a TFVE group. It was anticipated that the styrenic group would undergo cationic polymerization, while there is no literature information about the reactivity of the latter under the same condition. Our experimental results confirmed the high selectivity of the two vinyl groups during cationic polymerization. Specifically, the styrenic group readily polymerized, whereas the TFVS group remained intact. This selectivity enables the preparation of vulcanizable SIBS by incorporating a TFVE moiety into the glassy segment through the copolymerization of TFVS and styrene.

RESULTS AND DISCUSSION

The overall synthetic route for vulcanizable SIBS is based on living cationic polymerization using 1-(*tert*-butyl)-3,5-bis(2-methoxypropan-2-yl)benzene (DicumOMe) as the initiator and $TiCl_4$ as the catalyst.[11] The polymerization was performed in a mixture of dichloromethane (DCM) and methyl cyclohexane (MeChx), with additives of DMAc as the carbocation stabilizer and D*t*BP as the proton trap. The functional group for cross-linking, i.e., trifluorovinyl ether, was introduced by copolymerization of styrene and TFVS, as shown in Scheme 1.

https://doi.org/10.1021/acs.macromol.5c01045
Macromolecules 2025, 58, 9373−9386

Scheme 2. Synthetic Routes to 1-((1,2,2-Trifluorovinyl)oxy)-4-vinylbenzene (TFVS) in the Literature[31,32,53] and in the Present Study

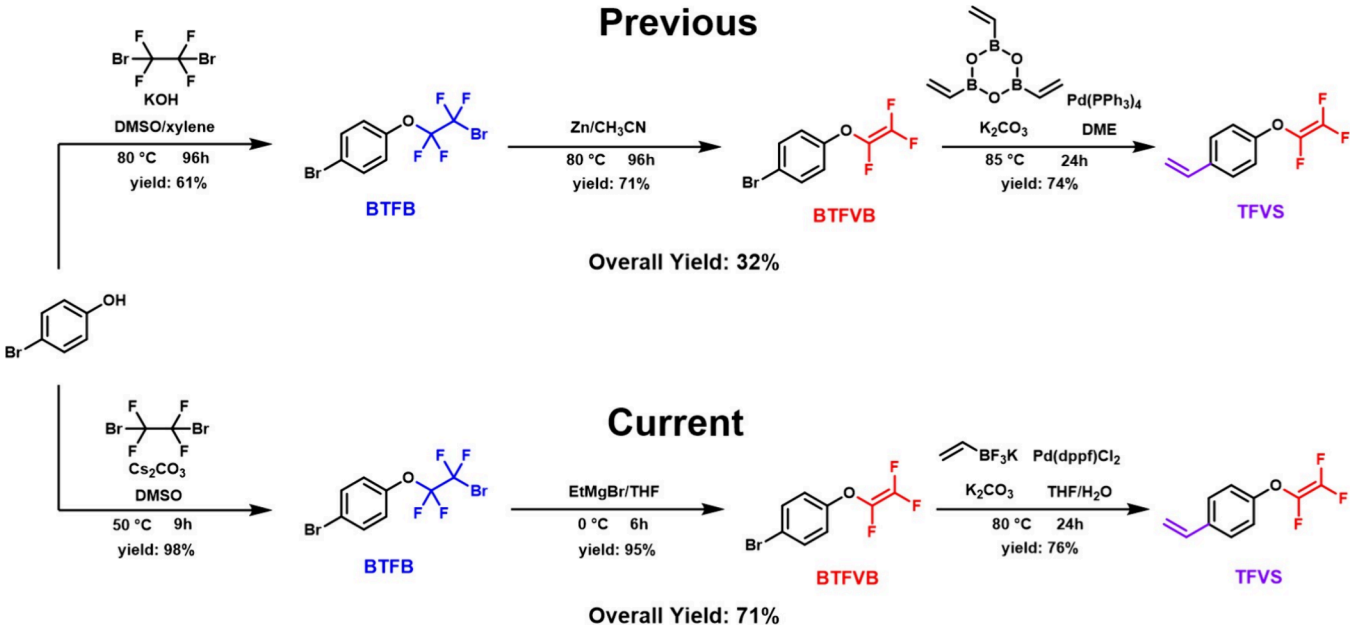

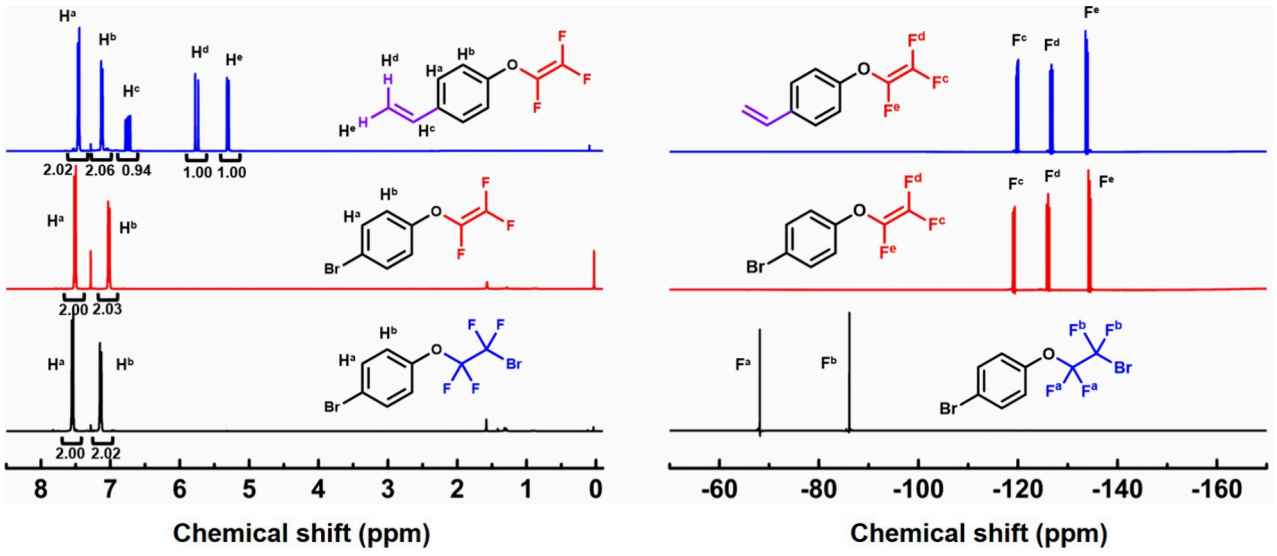

Figure 1. ^{1}H (left) and ^{19}F (right) NMR spectra of the intermediate and final products in the synthesis of TFVS.

It is important that the trifluorovinyl ether group of TFVS remains stable while the vinyl group undergoes cationic (co)polymerization. We first synthesized TFVS and investigated the selectivity of the two double bonds toward the cationic polymerization.

Synthesis of the Cross-Linker. The cross-linker TFVS was synthesized through a three-step process starting from nucleophilic substitution of 1,2-dibromotetrafluoroethane by 4-bromophenol and elimination of HF from the resulting ether, followed by the Suzuki coupling reaction between potassium vinyltrifluoroborate and the aromatic bromide, as shown in Scheme 2. The synthesis of TFVS was previously reported by Spraul and co-workers for the investigation of substituent effects on the cycloaddition reactivity of the trifluorovinylether group.[53] To our knowledge, however, the compound has not been used as a monomer for polymerization. In the present study, we modified the synthetic process by using an optimized method for each step as discussed below and achieved an overall yield as high as 71%.

The nucleophilic substitution reaction was conducted in DMSO at 50 °C in the presence of 1.5 equiv of Cs_2CO_3, a condition optimized by Li and co-workers.[54] The uses of Cs_2CO_3 as the catalyst and DMSO as the solvent are critical to avoid side reactions, giving high yield (~98%) of the etherification product, 1-bromo-4-(2-bromo-1,1,2,2-tetrafluoroethoxy)benzene (BTFB), which was superior to previously reported 61% using KOH and the mixed solvent of DMSO/xylene.[55] The product of the optimized condition can be used directly in the following reaction without purification.

The elimination reaction of BTFB was performed in the presence of a Grignard reagent, EtMgBr, at 0 °C in THF, resulting in bromoaryl trifluorovinyl ether 1-bromo-4-((1,2,2-trifluorovinyl)oxy)benzene (BTFVB). The use of EtMgBr for elimination was reported by Hu and Liu in the synthesis of

https://doi.org/10.1021/acs.macromol.5c01045
Macromolecules 2025, 58, 9373−9386

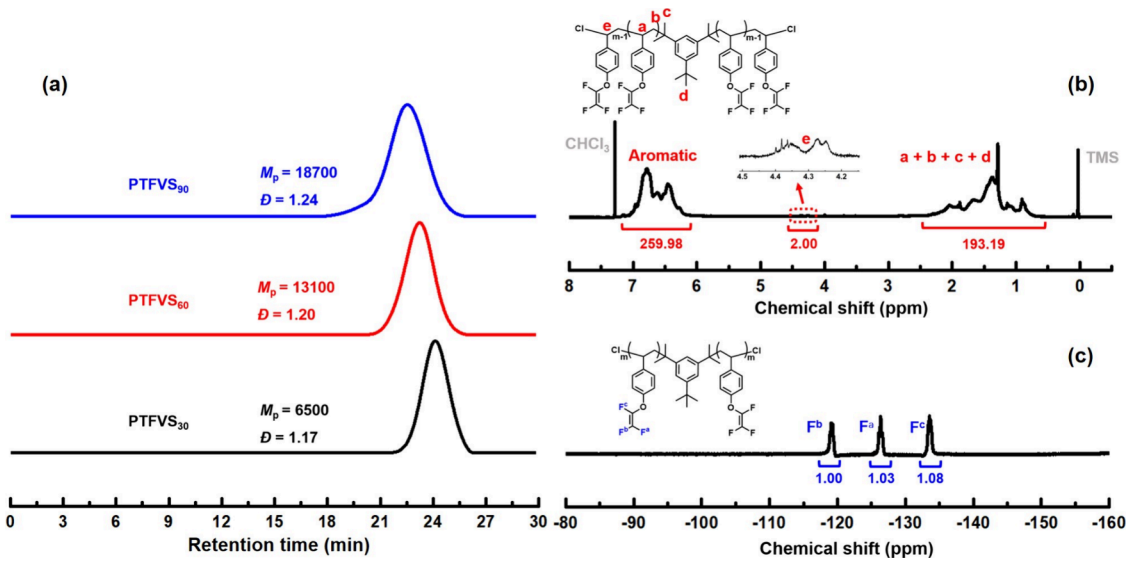

Figure 2. (a) SEC curves of the PTFVS homopolymer terminated at 5 min; (b) ^{1}H and (c) ^{19}F NMR spectra of PTFVS.

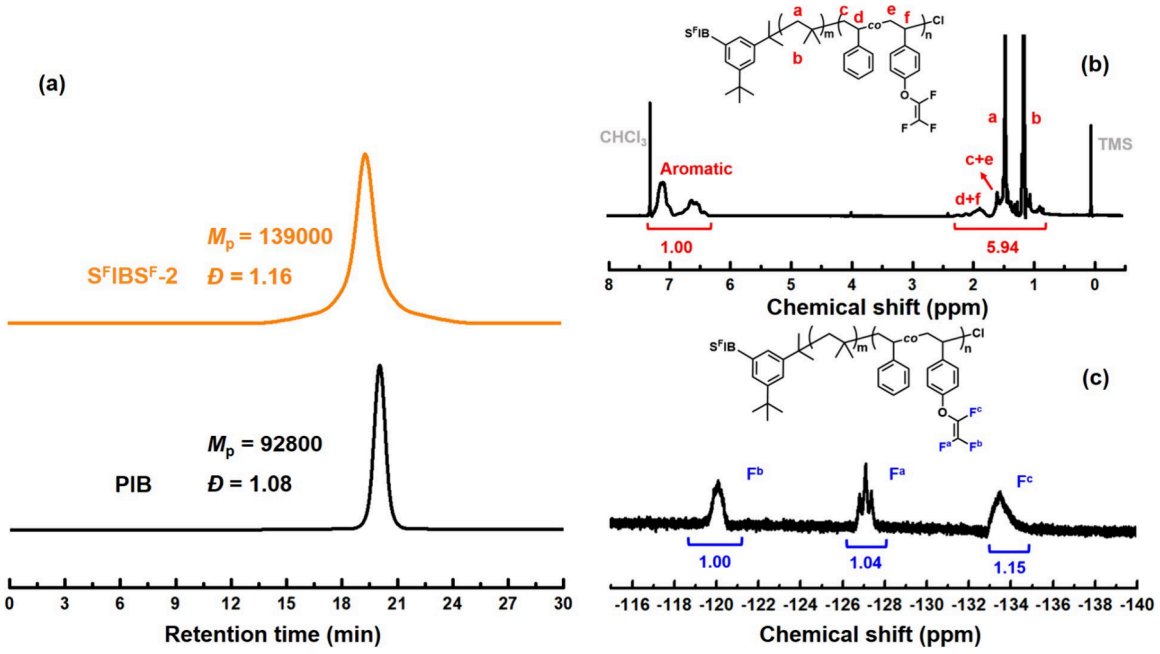

Figure 3. (a) SEC curves of PIB and the triblock copolymer, S^{F}IBS^{F}-2; (b) ^{1}H and (c) ^{19}F NMR spectra of S^{F}IBS^{F}-2.

various aryl trifluorovinyl ethers.[56] The yield was around 95% in contrast to that by the method using a zinc catalyst.[55]

The Suzuki coupling reaction was carried out using BTFVB and potassium vinyltrifluoroboronate as the coupling agent. The latter is commercially available, whereas the coupling agent used in ref 54 (2,4,6-trivinylcyclotriboroxane) had to be prepared separately. The yield of the coupling reaction was 76%, giving an overall yield of 71% for the three-step reaction.

Figure 1 shows the ^{1}H and ^{19}F NMR spectra of the products during the synthetic process. The product of the nucleophilic substitution shows two signals of aromatic protons at chemical shifts δ = 7.13 and 7.53 ppm. Meanwhile, two signals for fluorine atoms appear as singlets at −68.31 and −86.14 ppm, respectively. After the elimination reaction, the aromatic signals shift upfield to δ = 7.02 and 7.49 ppm, whereas three signals for ^{19}F peaks appear at δ = −134.62, −119.74, and −126.28 ppm, all as a quartet, for −OC*F*═, ═C*F*F (*cis*), and ═CF*F*(*trans*), respectively. The final product after Suzuki coupling, TFVS, shows olefinic signals at δ = 5.24 (e), 5.72 (d), and 6.69 ppm (c) in addition to the aromatic signals at δ = 7.01 (b) and 7.40 (a) ppm, while the signals of ^{19}F remain almost unchanged. All of the integration values are consistent to the molecular formulas. Furthermore, ^{13}C NMR spectra of TFVS also confirmed the successful synthesis of the target molecule TFVS (Figure S1).

Homopolymerization of TFVS. Since TFVS has never been used as a monomer for cationic polymerization, we first investigated the reactivity of the two double bonds under similar conditions to that in the subsequent block copolymer synthesis. The living cationic polymerization was conducted with the regulation of reversible activation/deactivation of carbocationic species by $TiCl_4$.[11] Dicumyl ether was used as the initiator, while DMAc and D*t*BP were used as an electron-donating additive and a proton trap, respectively, as shown in

https://doi.org/10.1021/acs.macromol.5c01045
Macromolecules 2025, 58, 9373−9386

Table 1. Triblock Copolymers SIBS and S^FIBS^F Prepared by Living Cationic Polymerization[a]

		PIB		triblock			
run	sample	M_p	M_w/M_n	M_p	M_w/M_n	$W_{PS+PTFVS,NMR}$(%)	TFVS feeding (wt %)
1	S^FIBS^F-2	92,800	1.08	139,000	1.16	36.9	2.0
2	S^FIBS^F-4	92,600	1.11	138,000	1.22	37.8	4.0
3	S^FIBS^F-6	94,000	1.13	141,000	1.24	38.6	6.0
4	SIBS	91,900	1.11	137,000	1.26	36.2	0

[a]Reaction conditions: $[IB]_0$ = 1.42 M, $[I]_0$ = 1.29 mM, $[DtBP]_0$ = 2.83 mM, $[DMAc]_0$ = 1.29 mM, $[TiCl_4]_0$ = 51.6 mM, $[St+TFVS]_0$ = 0.4 M for runs 1−3, $[St]_0$ = 0.37 M for run 4, in 60/40 (v/v) MeChx/DCM cosolvents, −80 °C.

Scheme S1. Upon addition of a dichloromethane solution of $TiCl_4$, the reaction mixture turned orange in color, indicating the initiation of the polymerization. The conversion of the styrenic group of TFVS, as determined by ^{1}H NMR spectrometry, reached nearly completion within 5 min (Figure 2b). Extending the reaction time to 10 min led to gelation of the system. However, the result of ^{19}F NMR spectrometry shows that the trifluorovinyl group remained intact during polymerization and gelation (Figure 2 and Figure S2), as the ^{19}F signals δ = −133.56, −119.29, and −126.30 ppm remain almost the same as those in the TFVS monomer. Therefore, the gelation at the later stage of cationic polymerization of TFVS is ascribed to the electrophilic reaction of the carbocation living chain ends to the phenyl side groups.

Figure 2 and Table S1 show SEC results of TFVS cationic polymerization products terminated at 5 min with different feed amounts of the initiator. It is clear that all of the products exhibit a single peak and the molecular weight is proportional to the ratio of the monomer to initiator, indicating that the polymerization proceeds via a controlled/"living" mode.

Synthesis of the Triblock Copolymer Poly(styrene-*co*-TFVS)-*b*-polyisobutylene-*b*-poly(styrene-*co*-TFVS) (S^FIBS^F). Sequential living cationic polymerization of IB and styrene/TFVS initiated by DicumOMe was performed to prepare the S^FIBS^F triblock copolymer. The reaction conditions were similar to those previously reported for the synthesis of SIBS.[11] The polymerization and cross-initiation were indicated by the color change from pale yellow to dark red upon addition of styrene/TFVS to the polymerization of isobutylene. The viscosity during the whole process increased remarkably up to a soft gel-like substance with a deep color. The reaction was quenched with methanol, accompanied by a gradual change to a colorless solution.

The block copolymerization process was monitored by using SEC and NMR analysis on samples taken from the system at different times (Figure 3 and Figure S3). A clear shift of the SEC peak is observed from the first block (PIB) at M_p = 92,800 to the final product at M_p = 139,000, indicating a living character of the polymerization. The peak of PIB is narrow and unimodal, while a shoulder is present in the peak of the final product (Figure S3). The shoulder broadens the molecular weight distribution of S^FIBS^F and is ascribed to chain branching through electrophilic attack of the living cationic chain ends to the side phenyl groups of styrenic repeating units. The same phenomenon was reported for the preparation of SIBS.[5,7] The chain branching can be circumvented by quenching the polymerization at an earlier time, e.g., 30 min instead of 40 min.

In order to investigate the distribution of TFVS units along the hard segment, a model copolymerization of styrene and TFVS was conducted at the same monomer feed ratio as that used in the synthesis of S^FIBS^F. The reaction was monitored by ^{1}H NMR spectroscopy using toluene as the internal standard, and the kinetic plots of both monomers are presented in Figure S4. The polymerization proceeded in two stages. The first stage was a rapid polymerization period within the initial 40 s, followed by slower first-order consumption of monomers. This particular kinetics is ascribed to larger ionization rates of the initiator relative to that of the polymer chain end, as suggested by Storey and Thomas in a study of the cationic copolymerization of styrene and isobutylene.[57] In both stages, styrene was consumed faster than TFVS. The higher reactivity of the former than the latter can be attributed to the electron-withdrawing nature of the (trifluorovinyl)oxy substituent, which reduces the reactivity of TFVS.[33] This result indicates a slightly tapered content of TFVS units along the chain. Nevertheless, the distribution of TFVS is statistical so that it will not have a significant effect on the mechanical property of cross-linked SIBS products.

In ^{1}H NMR of the final product (Figure 3b), the methyl and methylene signals of the PIB segment are clearly observed at 1.14 (peak b) and 1.44 ppm (peak a). The methylene and methine protons of the PS and PTFVS backbone were observed at 1.49−1.70 ppm (peaks c + e) and 1.76−2.33 ppm (peaks d + f). The broad peaks at 6.41−7.25 ppm were assigned to the aromatic protons of the PS and PTFVS. In ^{19}F NMR spectra (Figure 3c), the fluorine signals are observed at −133.43 (F^c), −127.13 (F^a), and −120.06 ppm (F^b), almost the same as those in the monomer TFVS. No signal is present for the virtually expected fluoroalkyl group formed by otherwise possible polymerization of the trifluorovinyl moiety.

Three samples of S^FIBS^F were synthesized with similar molecular weights (~140,000 for the triblock and 92,000−94,000 for PIB) and varying weight contents of trifluorovinyl monomer feeding (2.0, 4.0, and 6.0% over the total feeding weight of monomers), as listed in Table 1. For reference, a sample of SIBS was synthesized under the same conditions but without TFVS. The composition of the copolymer is roughly estimated from the integrations of the aromatic and aliphatic signals in the ranges of 6.4−7.2 and 0.8−2.3 ppm, respectively, by the following equation:

$$W_{PS+PTFVS,NMR} = \frac{M_{St} \times \frac{A_{arom}}{5}}{M_{St} \times \frac{A_{arom}}{5} + M_{IB} \times \frac{A_{aliph} - \frac{3}{5}A_{arom}}{8}} \times 100\% \quad (1)$$

in which $W_{PS+PTFVS,NMR}$ represents the weight fraction of the hard segment (styrene and TFVS) and M_{St} and M_{IB} represent the molecular weight of the styrene and isobutylene, respectively. A_{arom} and A_{aliph} represent the integration values of the aromatic and aliphatic protons, respectively. The contributions of styrene and TFVS units to the aromatic signals are indistinguishable in ^{1}H NMR. The calculated

https://doi.org/10.1021/acs.macromol.5c01045
Macromolecules 2025, 58, 9373−9386

weight contents of the hard segment were around 37−38%, which were close to the feeding contents of styrene and TFVS.

Thermal Cross-Linking Reaction of S^FIBS^F. The cross-linking reaction was carried out by heating S^FIBS^F samples in a press vulcanizer at 180−200 °C for 30−60 min under an applied pressure of 5 MPa. Previous studies have reported that the trifluorovinyl group undergoes $[2\pi + 2\pi]$ thermal cycloaddition at temperatures around 160 °C.[34,53]

The dimerization of the trifluorovinyl moiety via thermal cycloaddition forms cross-linking points in the outer segments of the triblock copolymer (Scheme 3). After being cured, the samples were subjected to Soxhlet extraction to determine the gel content. As summarized in Table 2, the gel contents varying widely from 2.2 to 95.1% were obtained depending on the original content of trifluorovinyl groups in the precursor as well as the heating temperature and duration. A higher content of trifluorovinyl ether, elevated temperature, and prolonged heating period all contributed to an increased cross-linking degree.

Scheme 3. Dimerization of the Aromatic Trifluorovinyl Ether Moiety through Thermal Cycloaddition

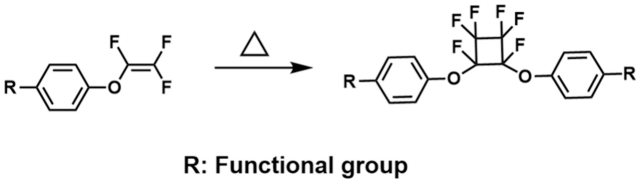

The cross-link density, D_c, defined as molar amounts of cross-links per unit volume of the sample, is determined by rheology measurement at 140 °C at the linear viscoelastic region according to the following equation:

$$G' = D_c N_A kT \quad (2)$$

where G' is the modulus at low frequency and T is the absolute temperature. It can be seen from Table 2 that D_c increases with the gel content yet not in a proportional way. It should be noted, however, that D_cs obtained here are only apparent values under ideal conditions of homogeneously distributed cross-links along the chain and throughout the sample. In comparison with the ideal scheme, the cross-links are localized only on the outer block of the copolymer in the present study. Therefore, the lengths of the elastic PIB strands between cross-links are very close to each other and are almost independent of the number of the cross-links because the outer blocks are relatively shorter.

Thermal and Mechanical Properties. Thermal properties of ^{F}x-S^FIBS^Fs were analyzed using DSC. Two glass transition temperatures, T_g, at −62 °C for the rubbery PIB segment and 105 °C for the glassy PS^F segment, were observed for all samples, as shown in Figure 4. These results are consistent to those of SIBS in this study and in the literature,[11] indicating that phase separation occurred in all samples including SIBS, S^FIBS^Fs, and ^{F}x-S^FIBS^Fs. It is also noticed from Figure 4 and Figure S5 that, upon cross-linking, the T_g of the hard segment slightly increased from 104.6 to 107.6 °C, while that of the soft segment increased from −64.9 to −62.2 °C. The unexpected increase in T_g of the soft segments may be a result of entrapment of PIB blocks in the network formed during the thermal curing process. We originally assume that the cross-linking occurred only in the hard domain. However, it turned out to be more complex because the cross-linking temperature was higher than the phase separation temperature, which may lead to a less well-developed morphology due to fixation of chains (to some extent) before phase separation.

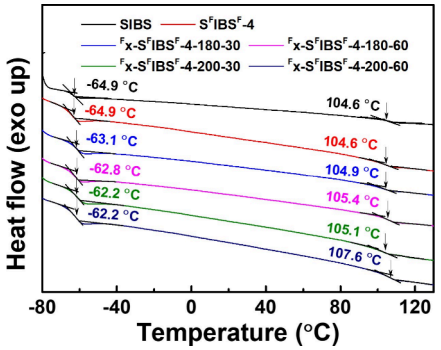

Figure 4. DSC results of SIBS, S^FIBS^F-4, and the corresponding cross-linked products, ^{F}x-S^FIBS^F, prepared at 180 and 200 °C for 30 and 60 min.

There have been literature reports on the effect of cross-linking in hard blocks on the glass transition temperature of the soft block in ABA-type block copolymers. To our knowledge, their conclusions depended on the conditions of the cross-linking process. Kawarazaki and co-workers observed that, when the hard domain was cured at lower temperatures under mild conditions such as photo-cross-linking, the T_g of the soft

Table 2. Curing Reaction Conditions and Analytical Results of the Cross-Linked Samples

sample	precursor	temperature	reaction time	gel content (%)	D_c (cross-linking density) (10^{-6} mol cm^{-3})
^{F}x-S^FIBS^F-2-180-30	S^FIBS^F-2	180 °C	0.5 h	2.2	24.0
^{F}x-S^FIBS^F-2-180-60		180 °C	1.0 h	7.6	24.9
^{F}x-S^FIBS^F-2-200-30		200 °C	0.5 h	9.4	25.1
^{F}x-S^FIBS^F-2-200-60		200 °C	1.0 h	18.3	30.4
^{F}x-S^FIBS^F-4-180-30	S^FIBS^F-4	180 °C	0.5 h	11.0	27.8
^{F}x-S^FIBS^F-4-180-60		180 °C	1.0 h	67.8	33.1
^{F}x-S^FIBS^F-4-200-30		200 °C	0.5 h	75.4	35.5
^{F}x-S^FIBS^F-4-200-60		200 °C	1.0 h	89.8	36.4
^{F}x-S^FIBS^F-6-180-30	S^FIBS^F-6	180 °C	0.5 h	42.5	29.7
^{F}x-S^FIBS^F-6-180-60		180 °C	1.0 h	71.9	36.8
^{F}x-S^FIBS^F-6-200-30		200 °C	0.5 h	83.2	37.7
^{F}x-S^FIBS^F-6-200-60		200 °C	1.0 h	95.1	45.5

https://doi.org/10.1021/acs.macromol.5c01045
Macromolecules 2025, 58, 9373−9386

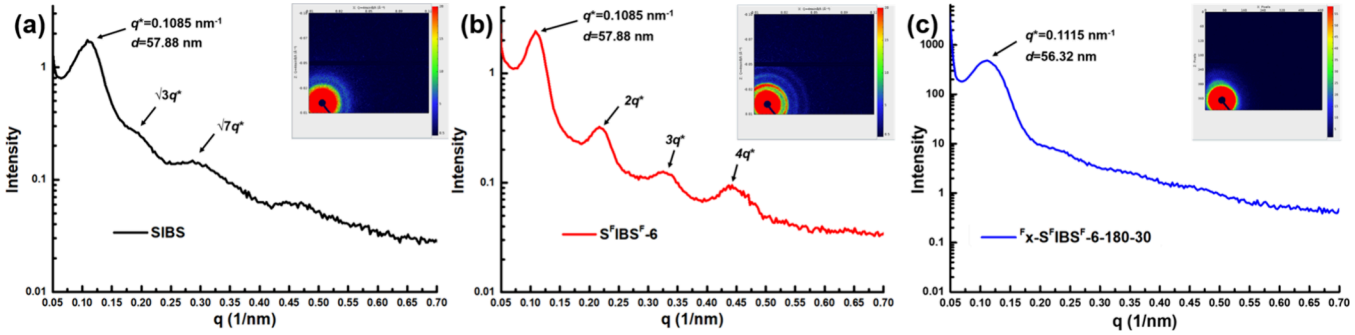

Figure 5. 1D and 2D SAXS profiles of SIBS (a), S^{F}IBS^{F}-6 (b), and ^{F}x-S^{F}IBS^{F}-6-180-30 (c).

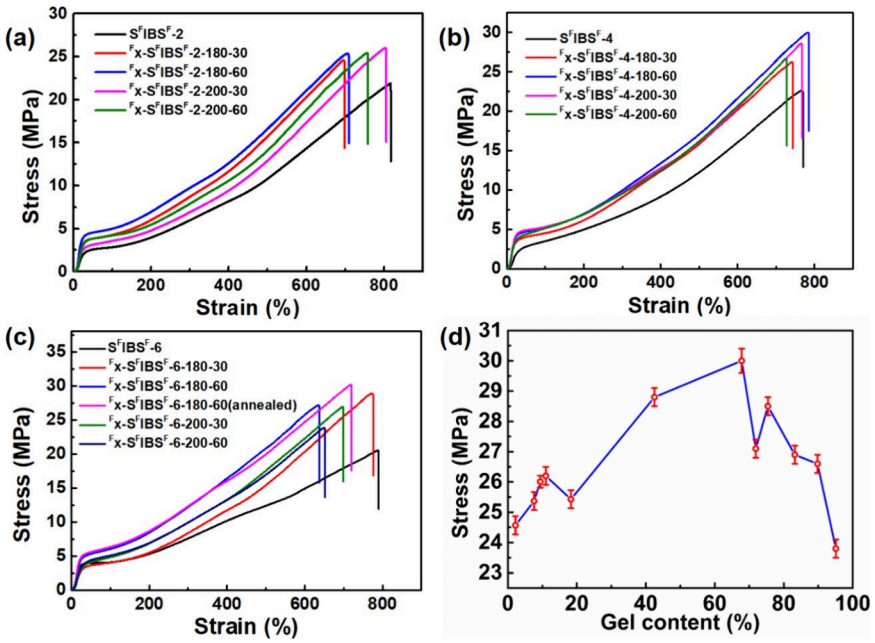

Figure 6. Stress−strain curves of S^{F}IBS^{F}s and ^{F}x-S^{F}IBS^{F}s cross-linked at 180 and 200 °C for 30 and 60 min (as indicated in the sample names) (a−c) and variation of tensile strength of ^{F}x-S^{F}IBS^{F}s along with different gel contents (d).

block was decreased, which was ascribed to the stretching of the end part of the soft segment by the cross-linking.[58] In another study, an increase in T_g of the soft segment was observed upon cross-linking of the hard block of an acrylic triblock copolymer through a Diels−Alder reaction at 120 °C.[59] Previously, McKenna and Park noticed that the size and confinement effects on the glass transition behavior of segments of block copolymers by cross-linking seemed to be material- and condition-specific.[60]

The evolution of morphology before and after cross-linking was analyzed using SAXS, as illustrated in Figure 5. All of the samples are prepared by hot pressing of a fine powder of the product after careful precipitation (slowly in methanol) and drying. The 2D patterns of SIBS and S^{F}IBS^{F}-6 exhibit distinct scattering rings, confirming the presence of microphase-separated structures. For SIBS, the peak positions of q^*, $\sqrt{3}q^*$, and $\sqrt{7}q^*$ suggest a hexagonally packed cylindrical (HPC) morphology, although the expected peak at $2q^*$ is absent. In contrast, S^{F}IBS^{F}-6 displays peaks at q^*, $2q^*$, $3q^*$, and $4q^*$, indicative of a lamellar (LAM) morphology. The domain spacing ($d = 2\pi/q$) of the microphase-separated structures was calculated to be 57.88 nm for both SIBS and S^{F}IBS^{F}-6, coincidentally. The observed difference in morphologies of SIBS and S^{F}IBS^{F}-6 may arise from slight compositional variation or the incorporation of TFVS units in the latter. The cross-linked sample, ^{F}x-S^{F}IBS^{F}-6-180-30 (Figure 5c), exhibits, however, only a broad peak at $q^* = 0.1115$ nm^{-1}. This suggests that while microphase separation occurred, the development of a well-defined morphology was hindered by the constraints of the cross-linked network. The estimated domain spacing decreased to 56.32 nm, which was slightly smaller than the uncross-linked sample. This trend agreed with the literature report for ABA-type block copolymers with cross-linked hard A segments.[61]

The stress−strain curves of S^{F}IBS^{F}s and ^{F}x-S^{F}IBS^{F}s are presented in Figure 6. All of the samples exhibit typical stress hardening behavior of an elastomer after passing a yield point at approximately 20% strain. The plastic to rubber transition was previously attributed to morphological changes in block copolymers exhibiting the LAM phase, in which the yield points correspond to the irregular deformation of the lamellar domains involving shearing, destruction, and orientation of the lamellae.[62] The effect of cross-linking is obvious from the improvement of the modulus of the hard phase and the yield stress relative to the uncross-linked samples in the initial plastic deformation stage. The network formation in the hard phase

https://doi.org/10.1021/acs.macromol.5c01045
Macromolecules 2025, 58, 9373−9386

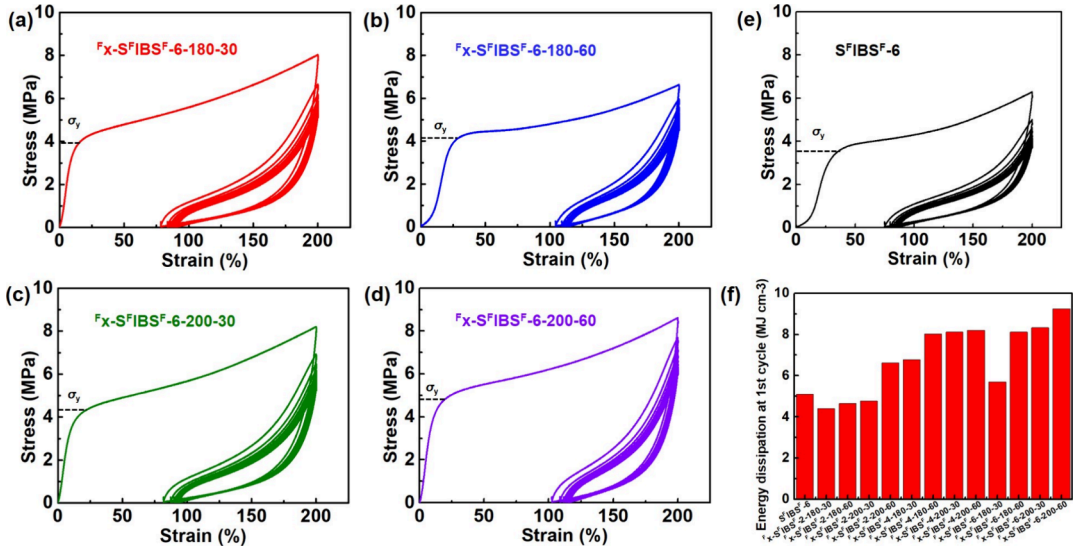

Figure 7. Mechanical hysteresis of 200% strain for 10 cycles of (a) ^{F}x-S^{F}IBS^{F}-6-180-30, (b) ^{F}x-S^{F}IBS^{F}-6-180-60, (c) ^{F}x-S^{F}IBS^{F}-6-200-30, (d) ^{F}x-S^{F}IBS^{F}-6-200-60, and (e) S^{F}IBS^{F}-6; (f) energy dissipation in the first cycle for S^{F}IBS^{F}-6 and ^{F}x-S^{F}IBS^{F} at various cross-linker contents, cross-linking temperatures, and time periods as indicated in the sample names.

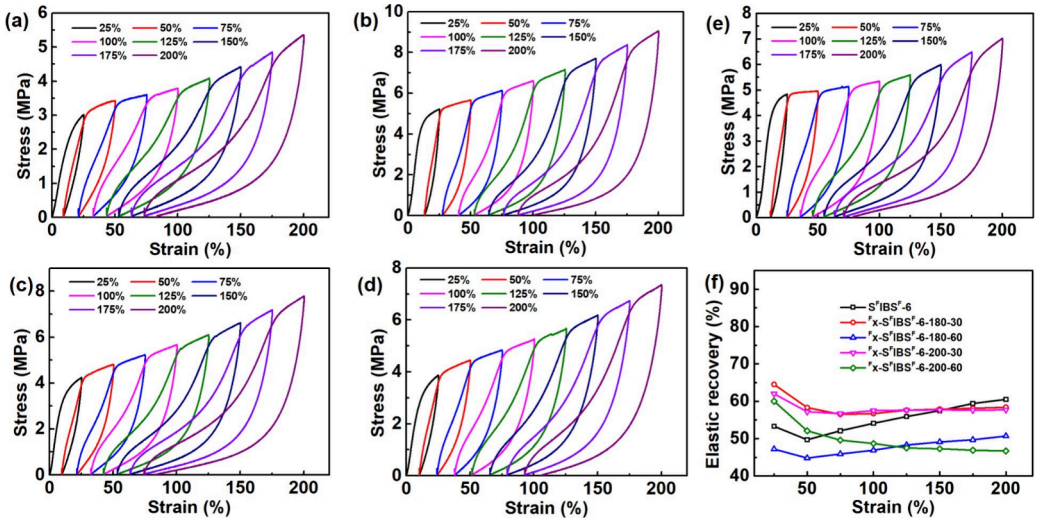

Figure 8. Curves of cyclic elastic recovery tests with progressive maximal strain from 25 to 200%. (a) ^{F}x-S^{F}IBS^{F}-6-180-30, (b) ^{F}x-S^{F}IBS^{F}-6-180-60, (c) ^{F}x-S^{F}IBS^{F}-6-200-30, (d) ^{F}x-S^{F}IBS^{F}-6-200-60, and (e) S^{F}IBS^{F}-6 and (f) elastic recovery values of all samples during the tests versus maximum strain from 25 to 200%.

therefore increases the overall tensile strength from, for example, 20.5 MPa (for the reference, S^{F}IBS^{F}-6) to 28.8 MPa (for ^{F}x-S^{F}IBS^{F}-6-180-30) after cross-linking. Similar improvements have also been observed in the S^{F}IBS^{F}-2 and S^{F}IBS^{F}-4 series. Further annealing of ^{F}x-S^{F}IBS^{F}-6-180-60 at 110 °C for 48 h leads to a marginal increase in stress at break from 27.2 MPa (without annealing) to 30.2 MPa (Figure 6c). Nevertheless, the elongations of the cross-linked samples are reduced to the range of 650−800% due to the fixation of the hard segment.

It is also noted that the increase in tensile strength depends on the cross-linking degree. There exists an optimal value of degree of cross-linking, as indicated by the gel fraction (68%), with the maximum stress at 30 MPa (Figure 6d). A further increase in cross-linking leads to a decline in tensile strength down to 23.8 MPa for 95.1% gel content. This is ascribed to overcross-linking that disrupts the subsequent microphase separation. The defects in microdomains in turn lead to earlier fracture of the sample due to the stress concentration. Therefore, cross-linking and microphase separation concurrently determine the mechanical property.

The mechanical hysteresis of ^{F}x-S^{F}IBS^{F}s was investigated through 10 cyclic tensile tests conducted at a stretch speed of 40 mm/min and a strain of 200%. As shown in Figure 7 and Figures S6 and S7, significant hysteresis is observed primarily in the first cycle, which is attributed mainly to irreversible deformation of the lamellar glassy domain. In subsequent cycles, the hysteresis gradually decreases, exhibiting behavior characteristic of thermoplastic elastomers. This suggests that the hard domain becomes dispersed in the rubber matrix.

Furthermore, the energy dissipation of the first cycle approximately increases with the gel content (Figure 7f). This trend stems from higher yield stress and greater residual strain induced by a more densely cross-linked network, which consequently enlarges the area between the stretching and relaxation curves.

https://doi.org/10.1021/acs.macromol.5c01045
Macromolecules 2025, 58, 9373−9386

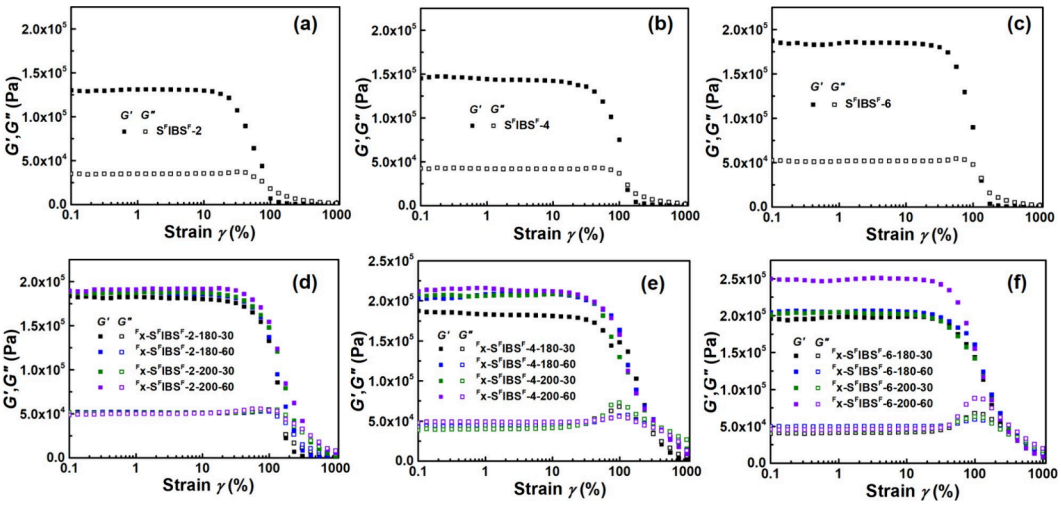

Figure 9. Storage modulus (G') and loss modulus (G'') as functions of oscillation strain for (a) S^FIBS^F-2, (b) S^FIBS^F-4, (c) S^FIBS^F-6, (d) ^Fx-S^FIBS^F-2s, (e) ^Fx-S^FIBS^F-4s, and (f) ^Fx-S^FIBS^F-6s at 140 °C. The frequency is fixed at 1 Hz.

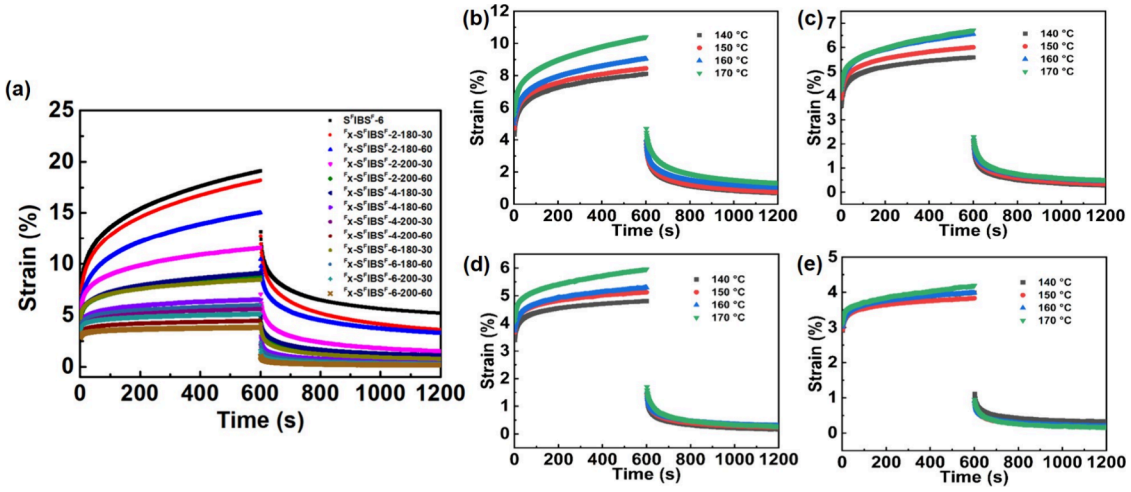

Figure 10. Creep−recovery results for all samples indicated in the figure. The tests are conducted at 150 °C with a shear stress of 5 kPa (a); creep−recovery results of (b) ^Fx-S^FIBS^F-6-180-30, (c) ^Fx-S^FIBS^F-6-180-60, (d) ^Fx-S^FIBS^F-6-200-30, and (e) ^Fx-S^FIBS^F-6-200-60 at different measuring temperatures.

All samples were further subjected to elastic recovery tests, in which the applied strains were incrementally increased to 25, 50, 75, 100, 125, 150, 175, and 200% at a velocity of 40 mm/min, and released to an unstressed length in each cycle. The results are given in Figure 8 and Figures S8 and S9. It is evident that the elastic recovery property is governed by the morphology, giving similar behavior for both the reference and the cross-linked samples. The strain recovery is maximal in the first cycle in the near-elastic region. Subsequent stretching causes the yielding of the specimen, although the yield point gradually diminishes, and the hysteresis loop increasingly resembles that of a typical elastomer. This observation further confirms destructive deformation within the plastic phase. Notably, a higher cross-linking degree, achieved by higher temperatures and longer heating times in the cross-linking reaction, leads to decreased elastic recovery (Figure 8f). This indicates that relaxation of the stretched chain is hindered by the network. Interestingly, when the stretched specimen was held for an interval between cycles for 1 and 5 min, the residual strain further diminished and the elastic recovery was enhanced, as shown in Figure S10. This indicates that part of the stretched chains slowly relaxed to its initial state and rebuilt part of the domains.

Storage and loss moduli (G' and G'') measured via strain sweeps are presented in Figure 9. The cross-linking causes obvious increases in the former. For example, the cross-linked sample, ^Fx-S^FIBS^F-6, exhibits a storage modulus in the range of 0.2−0.25 MPa, while the uncross-linked S^FIBS^F has G' less than 0.2 MPa. Similar results are obtained for the other two series of samples, S^FIBS^F-2 and S^FIBS^F-4, before and after cross-linking. When the cross-linking density is very high, such as in ^Fx-S^FIBS^F-6-200-60, the sample is more like a thermosetting material.

The creep tests were conducted at various temperatures under a shear stress of 5 kPa and a duration of 10 min, a condition ensuring a linear viscoelastic deformation determined via small-amplitude oscillatory shear strain scans (SAOS) shown in Figure 9. The creep results are presented in Figure 10 and Figures S11 and S12. Obviously, the uncross-linked precursor, S^FIBS^F-6, exhibits the highest creep strain (19%) at 150 °C among all samples (Figure 10a). All of the cross-linked samples show diminished creep. The viscoelastic

https://doi.org/10.1021/acs.macromol.5c01045
Macromolecules 2025, 58, 9373−9386

recovery increases for samples with a higher content of the cross-linking agent, elevated cross-linking temperatures (180−200 °C), and prolonged curing time. Samples containing 6% of TFVS units exhibit nearly complete recovery (lower curves in Figure 10a). In addition, for every sample, the creep became more significant as the testing temperature was higher (Figure 10b−e). These results demonstrate that ^{F}x-S^{F}IBS^{F}s possess superior dimensional stability and creep resistance compared to S^{F}IBS^{F}, owing to their chemically cross-linked network structure.

CONCLUSIONS

A novel trifluorovinyl ether based cross-linker, TFVS, was synthesized via an improved route and employed in the preparation of SIBS elastomers for on-demand curing. The two double bonds in TFVS are highly selective in cationic polymerization and thermal cross-linking reaction. While the vinyl group readily undergoes cationic polymerization, the trifluorovinyl ether group remains intact.

Block copolymers were synthesized through sequential living cationic polymerization of isobutylene and styrene/TFVS (at varying ratios) using DicumOMe/$TiCl_4$/D*t*BP/DMAc as the initiating/regulating system at −80 °C. The resulting products, S^{F}IBS^{F}s, underwent a cross-linking reaction via a [2 + 2] thermal cycloaddition reaction between trifluorovinyl ether moieties at temperatures ranging from 180 to 200 °C.

Compared to the noncross-linked S^{F}IBS^{F} reference, the cross-linked products demonstrated superior tensile strength and enhanced creep resistance, despite exhibiting higher hysteresis energy. The mechanical improvements are attributed to the formation of network, which endow a higher modulus to the hard phase and higher yield stress of the materials.

Although cross-linked S^{F}IBS^{F} is not reprocessable, it holds promise for biomedical applications where reprocessability is not a critical requirement. Given the established biocompatibility of SIBS, we anticipate that the strategy developed in the present study will find practical utility in biomedical materials development.

EXPERIMENTAL SECTION

Materials. All the materials used in this study were commercially available and used as supplied, unless otherwise stated. 4-Bromophenol (Adamas, ≥98%), 1,2-dibromotetrafluoroethane (Adamas, ≥99%), cesium carbonate (Cs_2CO_3, Greagent, ≥95%), dimethyl sulfoxide (DMSO, Adamas, anhydrous, ≥99%), EtMgBr (Adamas, 1.0 M solution in THF), diethyl ether (Et_2O, Greagent, ≥95%), potassium vinyltrifluoroborate (Adamas, ≥98%), potassium carbonate (K_2CO_3, Greagent, ≥99%), [1,1′-bis(diphenylphosphino)ferrocene]-dichloropalladium(II) (Pd(dppf)Cl_2, Adamas, ≥98%), tetrahydrofuran (THF, Adamas, anhydrous, ≥99%), 5-*tert*-butylisophthalic acid (Aladdin, ≥99%), methyl alcohol (MeOH, Adamas, anhydrous, ≥99%), sulfuric acid (H_2SO_4, Greagent, ≥95%), methylmagnesium bromide (Adamas, 1.0 M solution in THF), dichloromethane (DCM, Adamas, anhydrous, ≥99%), methylcyclohexane (MeChx, Adamas, anhydrous, ≥99%), triethylaluminum ($AlEt_3$; Adamas, 2.0 M solution in hexane), titanium tetrachloride ($TiCl_4$, J&K, 1.0 M solution in DCM), 2,6-di*tert*-butylpyridine (D*t*BP, Adamas, ≥98%), *N*,*N*-dimethylacetamide (DMAc, Adamas, anhydrous, ≥99%), and calcium hydride (CaH_2; Acros, ≥99%) were used as received. Isobutylene (IB, Weichuang Gases) was dried through columns packed with $CaSO_4$ and 4 Å molecular sieves; styrene (St, Adamas, ≥98%) and TFVS were distilled over CaH_2 in vacuum first and distilled over di-*n*-butylmagnesium before using it; the initiator DicumOMe was synthesized as the previously reported procedure.[5]

Measurements. ^{1}H, ^{13}C, and ^{19}F NMR spectra were recorded on a Bruker NMR instrument (400 MHz) using tetramethylsilane (TMS) as the interior reference and $CDCl_3$ as the solvent. Size-exclusion chromatography (SEC) analysis was performed on a Waters system equipped with a Waters 1525 binary HPLC pump, followed by three TSK gel columns (pore sizes of 15, 30, and 200 Å) and a Waters 2414 refractive index detector. The SEC system was calibrated by using narrow polystyrene standards. THF was used as the eluent, with a flow rate of 1.0 mL/min at 35 °C.

Room-temperature tensile tests were performed on dumbbell-shaped samples (ca. 35 mm × 2 mm × 1 mm) using an Instron 5966 tensile tester with a 1 kN load cell. The tensile speed was 40 mm/min. To ensure the accuracy of the results, several sample strips were tested for each sample. Cyclic tensile tests were performed at 40 mm/min for 10 cycles, both loading and unloading to 200% strain. A series of step cycle tensile tests was performed at a progressively higher strain. In each cycle, as the specimen reaches the required strain, the strain is gradually reduced at the same rate until the maximum stress is reached. The next required strain is then reached at the same rate. The elastic recovery (ER) values were obtained from the step cycle tensile tests.

$$\mathrm{ER} = \frac{\varepsilon - \varepsilon_{\mathrm{R}}}{\varepsilon} \times 100\% \tag{3}$$

where ε is the applied strain and ε_{R} is the residual strain after extension tests.

The dumbbell-shaped specimen was prepared as follows. For example, S^{F}IBS^{F}-6 was dissolved in THF (10% g/g). The solution was then cast slowly into a PTFE mold. After being cast, the mold surface was then covered with a piece of aluminum foil perforated with small holes to control the solvent evaporation rate. After ∼10 h, the exfoliated film was dried in a vacuum oven at 60 °C for 24 h and then hot pressed in a plate vulcanizer at 180 °C for 60 min. ^{F}x-S^{F}IBS^{F}-6-180-60 was obtained and annealed at 110 °C in a vulcanizer at a pressure of 5 MPa for 48 h.

The gel content was determined by Soxhlet extraction. The samples were placed in a stainless-steel mesh and immersed in toluene at 90 °C for 9 h. The extract was dried in a vacuum oven.

$$\text{gel content} = \frac{w_2}{w_1} \times 100\%$$

where w_1 is the weight of the sample before extraction and w_2 is the weight of the sample after extraction.

The cross-link density was determined by amplitude sweeps of rheology measurement. The cross-link density tests, small-amplitude oscillatory shear (SAOS), and shear creep−recovery tests were performed with a rotational rheometer (TA ARES-G2). The test was conducted according to methodologies previously described.[63,64]

Thermal properties of polymers were measured by a differential scanning calorimeter (DSC) (TA 250) under a nitrogen atmosphere at temperatures from −90 to 140 °C at a heating rate of 10 K/min.

The morphology was measured by small-angle X-ray scattering (SAXS). SAXS was carried out using a Xeuss 2.0 (Xenocs Co.) equipped with both a one-dimensional (1D) and two-dimensional (2D) detector. The sample-to-detector distance was 2500 mm. The X-ray wavelength used at all sample-to-detector distances was 1.1541 Å.

The specimens for the SAXS measurement were prepared as follows. For the reference, S^{F}IBS^{F}-6, the sample was prepared by solvent casting (THF, 10% g/g) into a PTFE mold. The mold surface was then covered with aluminum foil perforated with small holes to control the solvent evaporation rate. After ∼10 h, the exfoliated film was dried in a vacuum oven at 60 °C for 24 h and then annealed with two steps, i.e., 140 °C for 15 min and 110 °C for 24 h, in a vulcanizer at a pressure of 5 MPa. The above conditions did not cause cross-linking as demonstrated by complete dissolution of the sample and an almost identical GPC curve with the precursor.

For the cross-linking sample, ^{F}x-S^{F}IBS^{F}-6-180-30 was prepared by hot pressing a film of S^{F}IBS^{F}-6 obtained by solvent casting in a press

https://doi.org/10.1021/acs.macromol.5c01045
Macromolecules 2025, 58, 9373−9386

vulcanizer at 180 °C for 30 min. The obtained film was annealed at 110 °C in a vulcanizer at a pressure of 5 MPa for 48 h.

Synthesis of the Cross-Linker. 4-Bromophenol (17.3 g, 100.0 mmol) and Cs_2CO_3 (48.9 g, 150.0 mmol) were combined in a 1 L triple-neck flask; the system was pumped three times to replace it with an argon atmosphere. After adding 200 mL of DMSO and stirring for 1 h, 1,2-dibromotetrafluoroethane (52.0 g, 200.0 mmol) was added and the mixture was heated at 50 °C for 15 h. After completion of the reaction was monitored by TLC, the system was cooled to room temperature and 200 mL of deionized water was added. The mixture was extracted with DCM (100 mL × 3), and the organic phase was collected and washed with brine (100 mL × 3) and dried over anhydrous Na_2SO_4. The solvent was filtered, concentrated, and purified by column chromatography using petroleum ether as the eluent. The solvent was then concentrated by rotary evaporation to obtain BTFB as a colorless oil. Yield: 34.5 g (98%). ^{1}H NMR (400 MHz, $CDCl_3$, ppm): δ 7.53 (d, 2H, aromatic), 7.13 (d, 2H, aromatic). ^{19}F NMR (376 MHz, $CDCl_3$, ppm): δ −86.14 (t, 2F, −PhOCF_2CF_2Br), −68.31 (t, 2F, −PhOCF_2CF_2Br).

BTFP (28.2 g, 80.0 mmol) and THF (160 mL) were added to a three-neck flask, and the system was replaced with an argon atmosphere by pumping and exchanging three times; then, EtMgBr (120 mL, 150.0 mmol) was added dropwise at 0 °C. The mixture was then stirred for 5 h. After the completion of the reaction was monitored by ^{19}F NMR, deionized water (200 mL) was added to the mixture; then, the mixture was extracted with Et_2O (100 mL × 3) and the organic phase was collected and washed with brine (100 mL × 3) and dried over anhydrous Na_2SO_4. The solvent was filtered, concentrated, and purified by column chromatography using petroleum ether as the eluent. The solvent was then concentrated by rotary evaporation to obtain BTFVB as a colorless oil. Yield: 19.2 g (95%). ^{1}H NMR (400 MHz, $CDCl_3$, ppm): δ 7.49 (d, 2H, aromatic), 7.02 (d, 2H, aromatic). ^{19}F NMR (376 MHz, $CDCl_3$, ppm): δ −134.62 (dd, 1F, −PhOCFCF_2), −126.28 (dd, 1F, *trans*-CF_2CFOPh−), −119.74 (dd, 1F, *cis*-CF_2CFOPh−).

BTFVB (15.2 g, 60.0 mmol), potassium vinyltrifluoroborate (10.5 g, 78.0 mmol), Pd(dppf)Cl_2 (2.2 g, 3.0 mmol), K_2CO_3 (24.9 g, 180.0 mmol), and THF/H_2O (200 mL/20 mL) were added in a dry 500 mL round-bottom flask; after three freeze−thaw degassing, the mixture was heated to 85 °C and stirred for 20 h under argon. After cooling to room temperature, deionized water (200 mL) was added to the mixture, and then, the mixture was extracted with hexane (100 mL × 3) and the organic phase was collected and washed with brine (100 mL × 3) and dried over anhydrous Na_2SO_4. The solvent was filtered, concentrated, and purified by column chromatography using petroleum ether as the eluent. The solvent was then concentrated by rotary evaporation to obtain TFVS as colorless oil. Yield: 9.1 g (76%). ^{1}H NMR (400 MHz, $CDCl_3$, ppm): δ 7.40 (m, 2H, aromatic), 7.01 (d, 2H, aromatic), 6.69 (q, 1H, CH_2CHPh−), 5.72 (d, 1H, *cis*-CH_2CHPh−), 5.24 (d, 1H, *trans*-CH_2CHPh−). ^{19}F NMR (376 MHz, $CDCl_3$, ppm): δ −134.02 (dd, 1F, −PhOCFCF_2), −127.03 (dd, 1F, *trans*-CF_2CFOPh−), −119.56 (dd, 1F, *cis*-CF_2CFOPh−).

Synthesis of PTFVS. A Schlenk tube was evacuated and heated with an electric heat gun and then filled with argon, and the operation was repeated three times to remove the water oxygen adhering to the reaction bottles. The purified solvents (DCM, 2 mL, MeChx, 3 mL) and TFVS (195 mg) were added to the Schlenk tube and cooled at −80 °C. Then, D*t*BP (14 μL, 0.064 mmol), DMAc (3 μL, 0.032 mmol), and DicumOMe (9 mg, 0.032 mmol) were dissolved in 5 mL of cosolvents (DCM, 2 mL, MeChx, 3 mL) and added to the Schlenk tube; after stirring for 20 min, the co-initiators $TiCl_4$ (1.2 mL, 1 M in DCM, 1.2 mmol) were added to initiate polymerization. Five minutes later, 2 mL of precooled anhydrous methanol was added to quench the polymerization. The mixture was poured into excess methanol to precipitate and filtered, and then, the polymer was dissolved with toluene, followed by washing with a 10% NaOH solution; finally, the polymer was washed with deionized water several times until it was neutral, and then, the organic phase was added dropwise to excess methanol to precipitate; then, the polymer was dried in a vacuum oven.

Synthesis of SIBS. Four reaction bottles were connected serially to the vacuum line: one as a debridement bottle, one as a reaction bottle, one as an isobutylene collection bottle, and one as a styrene stock bottle. Four bottles were evacuated and heated with an electric heat gun and then filled with argon, and the operation was repeated three times to remove the water oxygen adhering to the reaction bottles. DCM (48 mL) and MeChx (72 mL) were added to the decontamination bottle, followed by the addition of triethylaluminum (6 mL, 2 M in hexane) for decontamination; after stirring for 30 min, all the solvents were flashed from the decontamination bottle to the reaction bottle and cosolvents (20 mL) were poured into the styrene stock bottle to which the amount of styrene required for polymerization was added. Then, the styrene stock bottle, the reaction bottle, and the isobutylene collection bottle were all cooled at −80 °C, and after opening the isobutylene gas valve to collect the desired amount of monomer, it was poured into the reaction bottle, which was subsequently filled with argon to positive pressure; then, D*t*BP (80 μL, 0.356 mmol), DMAc (15 μL, 0.162 mmol), and DicumOMe (45 mg, 0.162 mmol) were dissolved in 5 mL of cosolvents (DCM:MeChx = 4:6) and were added to the reaction bottle with a syringe; after stirring for 20 min, the co-initiator $TiCl_4$ (6.5 mL, 1 M in DCM, 6.5 mmol) was added to initiate polymerization. 50 min later, 2 mL of the reaction mixture was withdrawn from the reactor and quenched in excess methanol for determining the molecular weight of polyisobutylene, followed by the addition of precooled styrene solution, and when the polymerization was completed, it was quenched by the addition of precooled anhydrous methanol. The mixture was poured into excess methanol to precipitate and filtered, and then, the polymer was dissolved with toluene, followed by washing with a 10% NaOH solution; finally, the polymer was washed with deionized water several times until it was neutral, and then, the organic phase was added dropwise to excess methanol to precipitate; then, the polymer was dried in a vacuum oven at 70 °C for 3 days.

Synthesis of S^FIBS^F. The synthesis procedure for the PIB segment was the same as above; after the reaction of the PIB segment, the mixture of precooled styrene and TFVS was added into the reactor. When the polymerization was completed, it was quenched by the addition of precooled anhydrous methanol. The mixture was poured into excess methanol to precipitate and filtered, and then, the polymer was dissolved with toluene, followed by washing with a 10% NaOH solution; finally, the polymer was washed with deionized water several times until it was neutral, and then, the organic phase was added dropwise to excess methanol to precipitate; then, the polymer was dried in a vacuum oven at 70 °C for 3 days.

Synthesis of ^{F}x-S^FIBS^F. A sample (2.0 g) of the S^FIBS^F triblock copolymer was placed between two fluorinated polyimide films, and the films were placed between two flat metal plates. The resulting structure was placed in a press vulcanizer (180−200 °C) for 30−60 min with 5 MPa pressure applied and then cooled to room temperature, and the fluorinated polyimide films were removed from the metal plates. A small piece of the heat-treated polymer was placed in excess THF. The film remained insoluble overnight, indicating that it cross-linked.

■ ASSOCIATED CONTENT

Supporting Information

The Supporting Information is available free of charge at https://pubs.acs.org/doi/10.1021/acs.macromol.5c01045.

Additional experimental section, ^{19}F NMR, ^{13}C NMR, GPC, DSC, mechanical tests, and rheological measurement results (PDF)

■ AUTHOR INFORMATION

Corresponding Author

Junpo He − *The State Key Laboratory of Molecular Engineering of Polymers, Department of Macromolecular*

https://doi.org/10.1021/acs.macromol.5c01045
Macromolecules 2025, 58, 9373−9386

Science, Fudan University, Shanghai 200433, China; orcid.org/0000-0001-7754-1479; Email: jphe@fudan.edu.cn

Authors

Chunpeng Liu − *The State Key Laboratory of Molecular Engineering of Polymers, Department of Macromolecular Science, Fudan University, Shanghai 200433, China*

Qingquan Liu − *The State Key Laboratory of Molecular Engineering of Polymers, Department of Macromolecular Science, Fudan University, Shanghai 200433, China*

Yixin Liu − *The State Key Laboratory of Molecular Engineering of Polymers, Department of Macromolecular Science, Fudan University, Shanghai 200433, China;* orcid.org/0000-0001-9374-5981

Complete contact information is available at: https://pubs.acs.org/10.1021/acs.macromol.5c01045

Author Contributions

C.L.: Monomer synthesis, cationic polymerization, mechanical tests, SAXS measurements, writing of the original draft, and review and editing. Q.L.: Cationic polymerization. Y.L.: SAXS and analysis. J.H.: Conceptualization, data analysis, supervision, writing of the original draft, and review and editing.

Notes

The authors declare the following competing financial interest(s): A patent by J. H. and C. L. has been filed on the synthesis of S^FIBS^F and ^Fx-S^FIBS^F (No. CN118652364A).

■ ACKNOWLEDGMENTS

This work was subsidized by the National Natural Science Foundation of China (Grant No. 22071031).

■ REFERENCES

(1) Bates, F. S. Polymer-polymer phase behavior. *Science* **1991**, *251* (4996), 898−905.

(2) Leibler, L. Theory of Microphase Separation in Block Copolymers. *Macromolecules* **1980**, *13* (6), 1602−1617.

(3) Funaki, Y.; Kumano, K.; Nakao, T.; Jinnai, H.; Yoshida, H.; Kimishima, K.; Tsutsumi, K.; Hirokawa, Y.; Hashimoto, T. Influence of casting solvents on microphase-separated structures of poly (2-vinylpyridine)-block-polyisoprene. *Polymer* **1999**, *40* (25), 7147−7156.

(4) Kim, G.; Libera, M. Morphological development in solvent-cast polystyrene−polybutadiene−polystyrene (SBS) triblock copolymer thin films. *Macromolecules* **1998**, *31* (8), 2569−2577.

(5) Kwee, T.; Taylor, S. J.; Mauritz, K. A.; Storey, R. F. Morphology and mechanical and dynamic mechanical properties of linear and star poly(styrene-isobutylene-styrene) block copolymers. *Polymer* **2005**, *46* (12), 4480−4491.

(6) Sakurai, S.; Momii, T.; Taie, K.; Shibayama, M.; Nomura, S.; Hashimoto, T. Morphology transition from cylindrical to lamellar microdomains of block copolymers. *Macromolecules* **1993**, *26* (3), 485−491.

(7) Taylor, S. J.; Storey, R. F.; Kopchick, J. G.; Mauritz, K. A. Poly[(styrene-*co*-*p*-methylstyrene)-*b*-isobutylene-*b*-(styrene-*co*-*p*-methylstyrene)] triblock copolymers.: 1. Synthesis and characterization. *Polymer* **2004**, *45* (14), 4719−4730.

(8) Feldthusen, J.; Iván, B.; Müller, A. H. E. Synthesis of linear and star-shaped block copolymers of isobutylene and methacrylates by combination of living cationic and anionic polymerizations. *Macromolecules* **1998**, *31* (3), 578−585.

(9) Weidisch, R.; Gido, S.; Uhrig, D.; Iatrou, H.; Mays, J.; Hadjichristidis, N. Tetrafunctional multigraft copolymers as novel thermoplastic elastomers. *Macromolecules* **2001**, *34* (18), 6333−6337.

(10) Yu, J. M.; Dubois, P.; Jérôme, R. Poly [alkyl methacrylate-*b*-butadiene-*b*-alkyl methacrylate] triblock copolymers: Synthesis, morphology, and mechanical properties at high temperatures. *Macromolecules* **1996**, *29* (26), 8362−8370.

(11) Kaszas, G.; Puskas, J. E.; Kennedy, J. P.; Hager, W. G. Polyisobutylene-Containing Block Polymers by Sequential Monomer Addition. II. Polystyrene-Polyisobutylene-Polystyrene Triblock Polymers: Synthesis, Characterization, and Physical Properties. *J. Polym. Sci., Part A: Polym. Chem. Ed.* **1991**, *29* (3), 427−435.

(12) Cao, X.; Faust, R. Polyisobutylene-based thermoplastic elastomers. 5. Poly (styrene-*b*-isobutylene-*b*-styrene) triblock copolymers by coupling of living poly (styrene-*b*-isobutylene) diblock copolymers. *Macromolecules* **1999**, *32* (17), 5487−5494.

(13) Chen, X.; Iván, B.; Kops, J.; Batsberg, W. Block copolymers of styrene and *p*-acetoxystyrene with polyisobutylene by combination of living carbocationic and atom transfer radical polymerizations. *Macromol. Rapid Commun.* **1998**, *19* (11), 585−589.

(14) Everland, H.; Kops, J.; Nielsen, A.; Iván, B. Living carbocationic polymerization of isobutylene and synthesis of ABA block copolymers by conventional laboratory techniques. *Polym. Bull.* **1993**, *31*, 159−166.

(15) Puskas, J. E.; Kaszas, G. Polyisobutylene-based thermoplastic elastomers: A review. *Rubber Chem. & Technol.* **1996**, *69* (3), 462−475.

(16) Richter, D.; Arbe, A.; Colmenero, J.; Monkenbusch, M.; Farago, B.; Faust, R. Molecular motions in polyisobutylene: A neutron spin-echo and dielectric investigation. *Macromolecules* **1998**, *31* (4), 1133−1143.

(17) Storey, R. F.; Baugh, D., Iii Poly (styrene-*b*-isobutylene-*b*-styrene) block copolymers and ionomers therefrom: morphology as determined by small-angle X-ray scattering and transmission electron microscopy. *Polymer* **2000**, *41* (9), 3205−3211.

(18) Storey, R. F.; Chisholm, B. J.; Lee, Y. Synthesis and characterization of linear and three-arm star radial poly (styrene-*b*-isobutylene-*b*-styrene) block copolymers using blocked dicumyl chloride or tricumyl chloride/$TiCl_4$/pyridine initiating system. *Polymer* **1993**, *34* (20), 4330−4335.

(19) Storey, R. F.; Chisholm, B. J.; Masse, M. A. Morphology and physical properties of poly (styrene-*b*-isobutylene-*b*-styrene) block copolymers. *Polymer* **1996**, *37* (14), 2925−2938.

(20) Claiborne, T., III; Bluestein, D.; Schoephoerster, R. Development and evaluation of a novel artificial catheter-deliverable prosthetic heart valve and method for in vitro testing. *Int. J. Artif. Organs* **2009**, *32* (5), 262−271.

(21) El Fray, M.; Prowans, P.; Puskas, J. E.; Altstädt, V. Biocompatibility and fatigue properties of Polystyrene−Polyisobutylene−Polystyrene, an emerging thermoplastic elastomeric biomaterial. *Biomacromolecules* **2006**, *7* (3), 844−850.

(22) Pinchuk, L.; Wilson, G. J.; Barry, J. J.; Schoephoerster, R. T.; Parel, J.-M.; Kennedy, J. P. Medical applications of poly (styrene-block-isobutylene-block-styrene)("SIBS"). *Biomaterials* **2008**, *29* (4), 448−460.

(23) Wang, Q.; McGoron, A. J.; Bianco, R.; Kato, Y.; Pinchuk, L.; Schoephoerster, R. T. In-vivo assessment of a novel polymer (SIBS) trileaflet heart valve. *J. Heart Valve Dis.* **2010**, *19* (4), 499−505.

(24) Peppas, N. A.; Langer, R. New challenges in biomaterials. *Science* **1994**, *263* (5154), 1715−1720.

(25) Pinchuk, L.; Khan, I. J.; Martin, J. B.; Wilson, G. J.*Polyisobutylene-based thermoplastic elastomers for ultra long-term implant applications, Sixth World Biomaterials Congress* 2000.

(26) Pinchuk, L. A review of the biostability and carcinogenicity of polyurethanes in medicine and the new generation of'biostable'polyurethanes. *J. Biomater. Sci., Polym. Ed.* **1995**, *6* (3), 225−267.

(27) Puskas, J. E.; Chen, Y. Biomedical application of commercial polymers and novel polyisobutylene-based thermoplastic elastomers for soft tissue replacement. *Biomacromolecules* **2004**, *5* (4), 1141−1154.

(28) Puskas, J. E.; Chen, Y.; Dahman, Y.; Padavan, D. Polyisobutylene-based biomaterials. *J. Polym. Sci., Part A: Polym. Chem. Ed.* **2004**, *42* (13), 3091−3109.
(29) Ranade, S. V.; Richard, R. E.; Helmus, M. N. Styrenic block copolymers for biomaterial and drug delivery applications. *Acta Biomater.* **2005**, *1* (1), 137−144.
(30) Sheriff, J.; Claiborne, T. E.; Tran, P. L.; Kothadia, R.; George, S.; Kato, Y. P.; Pinchuk, L.; Slepian, M. J.; Bluestein, D. Physical Characterization and Platelet Interactions under Shear Flows of a Novel Thermoset Polyisobutylene-based Co-polymer. *Acs Appl. Mater. Inter.* **2015**, *7* (39), 22058−22066.
(31) Babb, D. A.; Boone, H. W.; Smith, D. W.; Rudolf, P. W. Perfluorocyclobutane aromatic ether polymers. III. Synthesis and thermal stability of a thermoset polymer containing triphenylphosphine oxide. *J. Appl. Polym. Sci.* **1998**, *69* (10), 2005−2012.
(32) Babb, D. A.; Ezzell, B. R.; Clement, K. S.; Richey, W. F.; Kennedy, A. P. Perfluorocyclobutane Aromatic Ether Polymers. *J. Polym. Sci., Part A: Polym. Chem. Ed.* **1993**, *31* (13), 3465−3477.
(33) Ji, J.; Narayan-Sarathy, S.; Neilson, R. H.; Oxley, J. D.; Babb, D. A.; Rondan, N. G.; Smith, D. W. [p-((trifluorovinyl)oxy)phenyl]-lithium: Formation, synthetic utility, and theoretical support for a versatile new reagent in fluoropolymer chemistry. *Organometallics* **1998**, *17* (5), 783−785.
(34) Smith, D. W.; Babb, D. A. Perfluorocyclobutane aromatic polyethers. Synthesis and characterization of new siloxane-containing fluoropolymers. *Macromolecules* **1996**, *29* (3), 852−860.
(35) Kim, B. G.; Kim, H. J.; Jang, J. H.; Cho, E. A.; Henkensmeier, D.; Kim, S. K.; Oh, I. H.; Hong, S. A.; Lim, T. H. Crosslinked monosulfonated poly(arylene ether) using cyclodimerization of trifluorovinyl ether groups for fuel cell applications. *Polym. Int.* **2011**, *60* (4), 685−691.
(36) Huang, R.; Yao, J.; Mu, Q.; Peng, D.; Zhao, H.; Yang, Z. Study on the Synthesis and Thermal Stability of Silicone Resin Containing Trifluorovinyl Ether Groups. *Polymers* **2020**, *12* (10), 2284.
(37) Yang, D.; Tong, L.; Li, Y.; Hu, J.; Zhang, S.; Huang, X. A novel well-defined amphiphilic diblock copolymer containing perfluorocyclobutyl aryl ether-based hydrophobic segment. *Polymer* **2010**, *51* (8), 1752−1760.
(38) Li, Y.; Zhang, S.; Tong, L.; Li, Q.; Li, W.; Lu, G.; Liu, H.; Huang, X. Perfluorocyclobutyl-based methacrylate monomers: Synthesis and radical polymerization. *J. Fluorine Chem.* **2009**, *130* (3), 354−360.
(39) Xu, B.; Yao, W.; Li, Y.; Zhang, S.; Huang, X. Perfluorocyclobutyl Aryl Ether-Based ABC Amphiphilic Triblock Copolymer. *Sci. Rep.* **2016**, *6*, 39504.
(40) Yao, W.; Li, Y.; Feng, C.; Lu, G.; Huang, X. Synthesis of amphiphilic ABA triblock copolymer bearing PIB and perfluorocyclobutyl aryl ether-containing segments via sequential living carbocationic polymerization and ATRP. *Polym. Chem.* **2014**, *5* (21), 6334−6343.
(41) Yao, W.; Li, Y.; Zhang, S.; Liu, H.; Huang, X. Novel perfluorocyclobutyl aryl ether-based well-defined amphiphilic block copolymer. *J. Polym. Sci., Part A: Polym. Chem. Ed.* **2011**, *49* (20), 4433−4440.
(42) Tong, L.; Shen, Z.; Zhang, S.; Li, Y.; Lu, G.; Huang, X. Synthesis and characterization of perfluorocyclobutyl aryl ether-based amphiphilic diblock copolymer. *Polymer* **2008**, *49* (21), 4534−4540.
(43) Li, Y.; Guo, H. Crosslinked poly(methyl methacrylate) with perfluorocyclobutyl aryl ether moiety as crosslinking unit: thermally stable polymer with high glass transition temperature. *RSC Adv.* **2020**, *10* (4), 1981−1988.
(44) Wang, J.; Sun, J.; Zhou, J.; Jin, K.; Fang, Q. Fluorinated and Thermo-Cross-Linked Polyhedral Oligomeric Silsesquioxanes: New Organic-Inorganic Hybrid Materials for High-Performance Dielectric Application. *Acs Appl. Mater. Inter.* **2017**, *9* (14), 12782−12790.
(45) Yuan, C.; Wang, J.; Jin, K.; Diao, S.; Sun, J.; Tong, J.; Fang, Q. Postpolymerization of Functional Organosiloxanes: An Efficient Strategy for Preparation of Low-*k* Material with Enhanced Thermostability and Mechanical Properties. *Macromolecules* **2014**, *47* (18), 6311−6315.
(46) He, F.; Gao, Y.; Jin, K.; Wang, J.; Sun, J.; Fang, Q. Conversion of a Biorenewable Plant Oil (Anethole) to a New Fluoropolymer with Both Low Dielectric Constant and Low Water Uptake. *ACS Sustainable Chem. & Eng.* **2016**, *4* (8), 4451−4456.
(47) Wang, J.; Jin, K.; Sun, J.; Fang, Q. Dendrimeric organosiloxane with thermopolymerizable − OCF = CF2 groups as the arms: synthesis and transformation to the polymer with both ultra-low *k* and low water uptake. *Polym. Chem.* **2016**, *7* (20), 3378−3382.
(48) Wang, J.; Zhou, J.; Jin, K.; Wang, L.; Sun, J.; Fang, Q. A New Fluorinated Polysiloxane with Good Optical Properties and Low Dielectric Constant at High Frequency Based on Easily Available Tetraethoxysilane (TEOS). *Macromolecules* **2017**, *50* (23), 9394−9402.
(49) Zhou, J.; Fang, L.; Wang, J.; Sun, J.; Jin, K.; Fang, Q. Post-functionalization of novolac resins by introducing thermo-cross-linkable − OCF = CF2 groups as the side chains: a new strategy for production of thermosetting polymers without releasing volatiles. *Polym. Chem.* **2016**, *7* (26), 4313−4316.
(50) Xin, Y.; Wang, J.; Jin, K.; Luo, Y.; Zhou, J.; Wang, Y.; Sun, J.; Zheng, S.; Fang, Q. A New Four-Arm Organosiloxane with Thermopolymerizable Trifluorovinyl ether Groups: Synthesis and Conversion to the Polymer with both Low Dielectric Constant and Low Water Uptake. *Macromol. Chem. Phys.* **2017**, *218* (13), 1700010.
(51) Ki, G.; Jang, K.-S.; Ka, J.-W.; Ahn, T. Synthesis and characterization of thermally curable 4-(1,2,2-trifluorovinyloxy)-benzoyl substituted poly(4-vinylphenol) for gate insulator in thin film transistor. *Mol. Cryst. & Liq. Cryst.* **2018**, *660* (1), 33−41.
(52) Zhou, J. F.; Tao, Y. Q.; Chen, X. Y.; Chen, X. R.; Fang, L. X.; Wang, Y. Q.; Sun, J.; Fang, Q. Perfluorocyclobutyl-based polymers for functional materials. *Mater. Chem. Front.* **2019**, *3* (7), 1280−1301.
(53) Spraul, B. K.; Suresh, S.; Jin, J. Y.; Smith, D. W. Synthesis and Electronic Factors in Thermal Cyclodimerization of Functionalized Aromatic Trifluorovinyl Ethers. *J. Am. Chem. Soc.* **2006**, *128* (21), 7055−7064.
(54) Li, J.; Qiao, J. X.; Smith, D.; Chen, B.-C.; Salvati, M. E.; Roberge, J. Y.; Balasubramanian, B. N. A practical synthesis of aryl tetrafluoroethyl ethers via the improved reaction of phenols with 1,2-dibromotetrafluoroethane. *Tetrahedron Lett.* **2007**, *48* (42), 7516−7519.
(55) Rizzo, J.; Harris, F. W. Synthesis and thermal properties of fluorosilicones containing perfluorocyclobutane rings. *Polymer* **2000**, *41* (13), 5125−5136.
(56) Liu, R.; Hu, J. Synthesis of Aryl Perfluorocyclopropyl Ethers via [2 + 1] Cyclopropanation Using $TMSCF_2Br$ Reagent. *Org. Lett.* **2022**, *24* (20), 3589−3593.
(57) Storey, R. F.; Thomas, Q. A. Quasi-Living Cationic Polymerization of Styrene and Isobutylene: Measurement of Run Number and Calculation of Apparent Rate Constant of Ionization by $TiCl_4$. *Macromolecules* **2003**, *36* (14), 5065−5071.
(58) Kawarazaki, I.; Hayashi, M.; Takasu, A. Extraction of intrinsic cross-linking effects of A hard domains on segmental motion of B soft block for ABA triblock copolymer-based elastomers by utilizing photo cross-linking. *Polymer* **2020**, *192*, No. 122343.
(59) Kavitha, A. A.; Singha, N. K. Smart "All Acrylate" ABA Triblock Copolymer Bearing Reactive Functionality via Atom Transfer Radical Polymerization (ATRP): Demonstration of a "Click Reaction" in Thermoreversible Property. *Macromolecules* **2010**, *43*, 3193−3205.
(60) Park, J.-Y.; McKenna, G. B. Size and confinement effects on the glass transition behavior of polystyrene/*o*-terphenyl polymer solutions. *Physical Rev. B* **2000**, *61*, 6667−6676.
(61) Jang, J.; Park, H.; Jeong, H.; Mo, E.; Kim, Y.; Yuk, J. S.; Choi, S. Q.; Kim, Y. W.; Shin, J. Thermoset elastomers covalently crosslinked by hard nanodomains of triblock copolymers derived from carvomenthide and lactide: tunable strength and hydrolytic degradability. *Polym. Chem.* **2019**, *10*, 1245−1257.

https://doi.org/10.1021/acs.macromol.5c01045
Macromolecules 2025, 58, 9373−9386

(62) Fujimura, M.; Hashimoto, T.; Kawai, H. Structural Change Accompanied by Plastic-to-Rubber Transition of SBS Block Copolymers. *Rubber Chem. Technol.* **1978**, *51*, 215−224.
(63) Fang, H.; Gao, X.; Zhang, F.; Zhou, W.; Qi, G.; Song, K.; Cheng, S.; Ding, Y.; Winter, H. H. Triblock Elastomeric Vitrimers: Preparation, Morphology, Rheology, and Applications. *Macromolecules* **2022**, *55* (24), 10900−10911.
(64) Xiao, Y. K.; Wang, W. J.; Li, B. G.; Liu, P. W. Thermoplastic Elastomer Based on Dynamically Cross-Linking Crystalline Macromers and Elastic Backbones. *Macromolecules* **2024**, *57* (4), 1788−1794.

https://doi.org/10.1021/acs.macromol.5c01045
Macromolecules 2025, 58, 9373−9386